Vertical and Lateral Mixing Processes Deduced from the Mediterranean Water Signature in the North Atlantic

JAN D. ZIKA

Climate and Environmental Dynamics and Laboratory, School of Mathematics and Statistics, University of New South Wales, Sydney, New South Wales, and Wealth from Oceans Flagship, CSIRO Marine and Atmospheric Research, Hobart, Tasmania, Australia

TREVOR J. MCDOUGALL

Wealth from Oceans Flagship, CSIRO Marine and Atmospheric Research, Hobart, Tasmania, Australia

(Manuscript received 29 November 2005, in final form 30 April 2007)

ABSTRACT

The conservation equations of heat, salt, and mass are combined in such a way that a simple relation is found between the known volume flux of Mediterranean Water entering the North Atlantic Ocean and the effects of lateral and vertical mixing processes. The method is a form of inverse method in which the only unknowns are the vertical and lateral diffusivities. For each isohaline contour on each neutral density surface the authors develop one equation in two unknowns, arguing that other terms that cannot be evaluated are small. By considering several such isohaline contours, the method becomes overdetermined for each density layer, and results are found for both the vertical and lateral diffusivity that vary smoothly in the vertical direction, giving some confidence in the method.

1. Introduction

The motivation for the present work dates back to the paper of McDougall (1984) in which the conservation equations of heat and salt were combined in a form that did not include the dianeutral advection, leaving a balance between lateral advection along a density surface and a specific combination of the effects of mixing of both heat and salt. This motivation will be described in this introduction for the advective form of the conservation equations. To make this approach workable as an inverse method in the ocean we need to implement this combination of conservation equations in the divergence form, and this is tackled in section 2.

The conservation equations for salinity S and conservative temperature Θ [which is proportional to potential enthalpy and represents the "heat content" per unit mass of seawater (McDougall 2003)] are

$$S_t|_\gamma + \mathbf{V}\cdot\boldsymbol{\nabla}_\gamma S + eS_z = h^{-1}\boldsymbol{\nabla}_\gamma\cdot(hK\boldsymbol{\nabla}_\gamma S) + (DS_z)_z \tag{1}$$

and

$$\Theta_t|_\gamma + \mathbf{V}\cdot\boldsymbol{\nabla}_\gamma\Theta + e\Theta_z = h^{-1}\boldsymbol{\nabla}_\gamma\cdot(hK\boldsymbol{\nabla}_\gamma\Theta) + (D\Theta_z)_z. \tag{2}$$

These equations have been written in the advective form and with respect to neutral density (γ^n) surfaces (Jackett and McDougall 1997) so that e is the vertical velocity through neutral density surfaces (i.e., the dianeutral velocity), and $\mathbf{V}$ is the thickness-weighted horizontal velocity obtained by temporally averaging the horizontal velocity between closely spaced neutral density surfaces. Similarly, the salinity and conservative temperature are the thickness-weighted values obtained by averaging between closely spaced pairs of neutral density surfaces (McDougall and McIntosh 2001). In these equations $h(x, y)$ is the thickness between two closely spaced neutral density surfaces. The mixing processes that appear on the right-hand sides are simply lateral mixing of passive tracers (with diffusivity K) along the density surfaces and vertical small-scale turbulent mixing (with diffusivity D). We have not

Corresponding author address: Jan D. Zika, CSIRO Marine and Atmospheric Research, Castray Esplanade, Hobart, TAS 7000, Australia.
E-mail: Jan.Zika@csiro.au

DOI: 10.1175/2007JPO3507.1

included double-diffusive convection or double-diffusive interleaving. Note that the distinction between conservative temperature and potential temperature is not central to this paper, and we will frequently refer to Θ as simply temperature.

Following McDougall (1984) we note that the temporal and spatial gradient of S and Θ along neutral tangent planes are related through the relevant thermal expansion coefficient ($\alpha = -\rho^{-1}\rho_{\Theta}|_{S,p}$) and haline contraction coefficient ($\beta = \rho^{-1}\rho_{S}|_{\Theta,p}$); that is,

$$\beta S_t|_\gamma = \alpha \Theta_t|_\gamma \quad \text{and} \quad \beta \nabla_\gamma S = \alpha \nabla_\gamma \Theta. \tag{3}$$

Strictly, these relations hold locally in neutral tangent planes, but here we will assume that they hold in neutral density surfaces since McDougall and Jackett (2005a,b) have shown that neutral density surfaces are everywhere almost tangent to neutral tangent planes.

The dianeutral advection term can be eliminated between (1) and (2) by multiplying the equations by Θ_z and S_z, respectively, and subtracting. On doing this and using (3) we find (similarly to McDougall 1984)

$$\begin{aligned} S_t|_\gamma + \mathbf{V}\cdot\nabla_\gamma S = {} & D\alpha g N^{-2}(\Theta_z S_{zz} - S_z\Theta_{zz}) \\ & + \frac{R_\rho}{(R_\rho - 1)} h^{-1}\nabla_\gamma \cdot (hK\nabla_\gamma S) \\ & - \frac{\alpha/\beta}{(R_\rho - 1)} h^{-1}\nabla_\gamma \cdot (hK\nabla_\gamma \Theta), \end{aligned} \tag{4}$$

where the buoyancy frequency N is defined by $N^2 = g(\alpha\Theta_z - \beta S_z)$, and $R_\rho \equiv \alpha\Theta_z/\beta S_z$ is the stability ratio of the vertical stratification. For completeness we also write down another important linear combination of (1) and (2), namely the one formed by cross-multiplying these equations by α and β, giving what might be loosely called the "density" conservation equation, or the equation for the dianeutral velocity, namely,

$$\begin{aligned} e = {} & D_z + DgN^{-2}(\alpha\Theta_{zz} - \beta S_{zz}) \\ & - KgN^{-2}(C_b\nabla_\gamma\Theta\cdot\nabla_\gamma\Theta + T_b\nabla_\gamma\Theta\cdot\nabla_\gamma p), \end{aligned} \tag{5}$$

where the cabbeling coefficient and the thermobaric coefficient (McDougall 1987, 1991a) are

$$C_b = \frac{\partial\alpha}{\partial\Theta} + 2\frac{\alpha}{\beta}\frac{\partial\alpha}{\partial S} - \frac{\alpha^2}{\beta^2}\frac{\alpha\beta}{\partial S} \quad \text{and} \quad T_b = \frac{\partial\alpha}{\partial p} - \frac{\alpha}{\beta}\frac{\partial\beta}{\partial p} \tag{6}$$

and represent the nonlinear nature of the equation of state of seawater.

The motivation for the present study comes from the rather simple balance in (4) between the lateral advection of salinity along isopycnals (the left-hand side) and the terms on the right that depend, respectively, on the vertical and lateral diffusivity. We describe this balance as "simple" for three reasons. First, (4) does not contain any dependence on the dianeutral velocity e or, second, on the vertical derivative of the vertical diffusivity D_z. Third, the term involving D in (4) is proportional to the curvature of the S–Θ diagram, which is much less subject to numerical noise caused by vertical heave than the second derivatives Θ_{zz} and S_{zz} in (1), (2), and (5); recall that

$$\frac{d^2S}{d\Theta^2} = \theta_z^{-3}(\Theta_z S_{zz} - S_z\Theta_{zz}). \tag{7}$$

For these three reasons we expect that the diapycnal mixing term in (4) can be evaluated from oceanographic data with less uncertainty than the diapycnal mixing and advection terms in (1) and (2). Quantitative knowledge of the flow out of the Mediterranean Sea into the North Atlantic Ocean, as described by Baringer and Price (1997), seems a suitable way of estimating the left-hand side of (4), so the eastern North Atlantic may be a region of the ocean where we could exploit the rather simple balance between advection and mixing processes, as given by (4), perhaps being able to perform an inverse model without the need to consider unknown reference level velocities, which are the traditional unknowns in oceanographic inversions. This idea is the motivation for the next section, in which we form rather specific combinations of the divergence forms of the basic conservation equations in order to arrive at an equation that satisfies the overall flux constraints over a finite volume but has the above three essential features of the "simple" curvature form conservation equation (4).

2. A careful linear combination of conservation equations

The three basic conservation (Boussinesq) equations, namely continuity, conservation of salinity, and conservation of conservative temperature, can be written in divergence form with respect to neutral density coordinates as (Griffies 2004)

$$h_t|_\gamma + \nabla_\gamma\cdot(h\mathbf{V}) + e^u - e^l = 0, \tag{8}$$

$$\begin{aligned} (hS)_t|_\gamma + \nabla_\gamma\cdot(h\mathbf{V}S) + e^uS^u - e^lS^l = {} & \nabla_\gamma\cdot(hK\nabla_\gamma S) \\ & + [DS_z]_l^u, \quad \text{and} \end{aligned} \tag{9}$$

$$\begin{aligned} (h\Theta)_t|_\gamma + \nabla_\gamma\cdot(h\mathbf{V}\Theta) + e^u\Theta^u - e^l\Theta^l = {} & \nabla_\gamma\cdot(hK\nabla_\gamma\Theta) \\ & + [D\Theta_z]_l^u. \end{aligned} \tag{10}$$

Here the superscripts u and l refer to the upper and lower interfaces bounding each layer and h is the vertical distance (layer thickness) between these bounding

density interfaces. In the above we have ignored double-diffusive convection in that the only diapycnal mixing is done with the same diffusivity for salinity as for conservative temperature. The last term in (9) [and in (10)] is the difference in the diapycnal flux of salt (and temperature) across the upper and lower density interfaces.

For each layer we will consider a series of control volumes bounded by the source of Mediterranean Water in the east and a series of contours of salinity and conservative temperature, S_0 and Θ_0. The S_0 and Θ_0 contours coincide because they are on a density surface. We multiply (8) by the constant values S_1 and Θ_1 (which we may well take to be different to S_0 and Θ_0, see below) and subtract these equations from (9) and (10), respectively obtaining

$$(h[S - S_1])_t|_\gamma + \nabla_\gamma \cdot (h\mathbf{V}[S - S_1]) = \nabla_\gamma \cdot (hK\nabla_\gamma S) + [DS_z]_l^u - e^u(S^u - S_1) + e^l(S^l - S_1) \quad \text{and} \tag{11}$$

$$(h[\Theta - \Theta_1])_t|_\gamma + \nabla_\gamma \cdot (h\mathbf{V}[\Theta - \Theta_1]) = \nabla_\gamma \cdot (hK\nabla_\gamma \Theta) + [D\Theta_z]_l^u - e^u(\Theta^u - \Theta_1) + e^l(\Theta^l - \Theta_1). \tag{12}$$

Here we have moved the dianeutral advection terms to the right-hand side since they only occur as a result of mixing processes and we wish to place all the mixing influences on the right-hand side. This step of subtracting the constant reference values S_1 and Θ_1 from the salinity and conservative temperature makes the divergence form of the conservation equations behave more like the advective forms (1) and (2). The resulting conservation equations for the anomaly variables are less sensitive to errors in the continuity equation (8) (McDougall 1991b; McIntosh and Rintoul 1997; Ganachaud and Wunsch 2000; Sloyan and Rintoul 2000). Since the lateral and vertical diffusion terms in (11) and (12) appear as gradients of S and Θ, we can regard (11) and (12) as exactly the same form of conservation equation as (9) and (10) except for the anomaly variables $[S - S_1]$ and $[\Theta - \Theta_1]$.

Now we ignore the temporal derivative term and spatially integrate (11) and (12) over the area from the Gulf of Cadiz to the S_0 contour (which almost exactly coincides with a Θ contour, Θ_0, on a neutral density surface). The volume flux into this layer from the Gulf of Cadiz is Q, which we will take as known from the work of Baringer and Price (1997). We will take the flow out across the S_0 contour to be cQ where we expect c to be not too different to unity because we will be considering contours that are not too distant from the Mediterranean outflow. In what follows we will assume that $0.7 < c < 1.0$. Taking the salinity and temperature of the Mediterranean outflow into this layer to be S_M and Θ_M, the area integrals of the left-hand sides of (11) and (12) {i.e., the area integrals of $\nabla_\gamma \cdot (h\mathbf{V}[S - S_1])$ and $\nabla_\gamma \cdot (h\mathbf{V}[\Theta - \Theta_1])$} are

$$\text{LHS\_S} = -Q[S_M - S_1] + cQ[S_0 - S_1] \quad \text{and} \tag{13}$$

$$\text{LHS\_}\Theta = -Q[\Theta_M - \Theta_1] + cQ[\Theta_0 - \Theta_1]. \tag{14}$$

The values of Q, S_M, and Θ_M represent the values of the Mediterranean outflow after it has reached its equilibrium depth and has begun to spread out neutrally into the interior of the North Atlantic. That is, the values will be chosen as representative of the flow after the intense dianeutral mixing and entrainment in the downslope flow has occurred. This is done so that our values of D and K represent interior mixing processes in the North Atlantic rather than representing intense mixing and dilution in the outflow plume. It is convenient to rearrange these equations as

$$\text{LHS\_S} = -FQ[S_M - S_0] \quad \text{and}$$

$$\text{LHS\_}\Theta = -FQ[\Theta_M - \Theta_0], \tag{15}$$

where

$$F = 1 - \frac{[S_1 - S_0]}{[S_M - S_0]}(1 - c) \approx 1 - \frac{[\Theta_1 - \Theta_0]}{[\Theta_M - \Theta_0]}(1 - c). \tag{16}$$

The second approximate equality follows because the salinity and temperature contrasts here are all measured along a neutral density surface and so are related though the thermal expansion coefficient and the saline contraction coefficient, which do not change substantially in this part of the North Atlantic. The values of S_1 and Θ_1 that we will choose will mean that F is little different to unity in our region of interest.

Now we come to the area integration of the right-hand sides of (11) and (12). The lateral diffusion terms become the lateral diffusion across the boundary of the control volume along the S_0 contour; namely,

$$\int_{S_0} hK\nabla_\gamma S \cdot \mathbf{n}\, dl \quad \text{and} \quad \int_{S_0} hK\nabla_\gamma \Theta \cdot \mathbf{n}\, dl, \tag{17}$$

where $\mathbf{n}$ is the outward unit vector in two dimensions, normal to the S_0 contour, and dl is the element of length along the S_0 contour.

Before area-integrating the diapycnal mixing and advection terms in (11) and (12), we rewrite these terms in (11) as

$$\frac{1}{2}(D^u + D^l)(S_z^u - S_z^l) - (e^u - e^l)\left[\frac{1}{2}(S^u + S^l) - S_1\right] - \frac{1}{2}(e^u + e^l)(S^u - S^l) + (D^u - D^l)\frac{1}{2}(S_z^u + S_z^l). \tag{18}$$

The first term, $0.5(D^u + D^l)(S_z^u - S_z^l)$, corresponds to the term DS_{zz} in (1), while the last term in (18) corresponds to $D_z S_z$ in (1). The first of the dianeutral advection terms in (18) does not have an analogous term in (1) while the other term, $-0.5(e^u + e^l)(S^u - S^l)$, corresponds to eS_z in (1). The next step in section 1 (where we were concerned with differential equations at a point) was to cross multiply the S and Θ equations by the vertical gradients of temperature and salinity. This step in section 1 eliminated the terms in $D_z S_z$ and eS_z, so simplifying the effects of diapycnal mixing into a single term that was proportional to the curvature of the vertical S–Θ cast. We follow a similar procedure here, with the aim of minimizing the influence of dianeutral advection and of the vertical variation of D on the final equation. Only the contribution from the first term in (18) will be significant in the final equation.

We form the area-averaged vertical difference variables

$$\Delta S \equiv \langle S^u - S^l \rangle \quad \text{and} \quad \Delta\Theta \equiv \langle \Theta^u - \Theta^l \rangle \tag{19}$$

and form ΔS times the area integral of (12) minus $\Delta\Theta$ times the area integral of (11), giving [using (15), (17), (18), and an equation corresponding to (18) for Θ]

$$FQ(\Delta\Theta[S_M - S_0] - \Delta S[\Theta_M - \Theta_0]) \approx \int_{S_0} hK(\Delta S \nabla_\gamma \Theta - \Delta\Theta \nabla_\gamma S) \cdot \mathbf{n}\, dl + A\langle D[(\Theta_z^u - \Theta_z^l)\Delta S - (S_z^u - S_z^l)\Delta\Theta] \rangle. \tag{20}$$

In addition, there are three other terms that should appear on the right-hand side of (20), namely, (A1)–(A3) of the appendix. We have omitted these terms here because in the appendix we show them to be negligible. Here A is the area from the Gulf of Cadiz to the salinity contour S_0, and the angle brackets indicate an area average over area A. This equation is the one used in this paper to deduce magnitudes for both the diffusivities D and K, given knowledge of FQ and of the hydrography in the eastern North Atlantic. We have used the symbol D in (20) for the average of the diapycnal diffusivity at the lower and upper interfaces, $0.5(D^u + D^l)$. In what follows we will take the diapycnal diffusivity D to be constant along a layer. It can also be noted from (20) that the numerical magnitudes that we obtain for both D and K in each layer are both directly proportional to the effective lateral advection, FQ.

Equation (20) corresponds to (4) in the advective approach, and notice that, like (4), (20) does not contain dianeutral advection and that diapycnal mixing enters proportionally to the curvature of the S–Θ diagram of the vertical water columns, averaged over the area A [since $(S_z^u - S_z^l)$ and $\Delta\Theta$ correspond to S_{zz} and Θ_z, respectively]. Vertical heave contributes considerable noise when evaluating S_{zz} and Θ_{zz} but, through cancellation, does not contribute significantly to the combination of terms $(\Theta_z S_{zz} - S_z \Theta_{zz})$, especially when the atlas data has been isopycnally averaged [as is the case with the atlas data of Gouretski and Koltermann (2004), which we use].

Equation (20) is, in fact, the conservation equation for the variable

$$\Delta S(\Theta - \Theta_1) - \Delta\Theta(S - S_1). \tag{21}$$

The choice of Θ_1 and S_1 as the volume-averaged conservative temperature and salinity of the control volume ensures that the term (A1) is minimized, while the choice of the ratio $\Delta S/\Delta\Theta$ as the ratio of the volume-averaged vertical gradients of salinity and temperature ensures that the vertical gradient of (21) is, on average, zero. This property minimizes the contribution of both dianeutral advection and the vertical gradient of D [terms (A2) and (A3)] to (20).

Note that at the level of maximum Mediterranean Water influence, where $\Delta S = 0$ (20) reduces to

$$FQ[S_M - S_0] = -K \int_{S_0} h \nabla_\gamma S \cdot \mathbf{n}\, dl - DA\langle S_z^u - S_z^l \rangle. \tag{22}$$

In comparing this equation with (the negative of) the area integral of the original salinity conservation equation (9), it can be seen that in this special case where $\Delta S = 0$ the price that has been paid for eliminating the influence of dianeutral advection across both the upper and lower interfaces is simply to introduce the factor F.

3. Diffusivities from hydrographic atlas data

Hydrographic data from the region of the North Atlantic near the Strait of Gibraltar have been taken from the atlas of Gouretski and Koltermann (2004). We have used the atlas at a horizontal resolution of ½° of longitude and latitude. Eight layers were chosen, bounded by nine neutral density surfaces, and in each of these layers we consider five areas from the Strait of Gibraltar to different salinity contours. In Fig. 1 we show S–Θ curves from the three locations (38°N, 350°E), (38°N, 345°E), and (38°N, 340°E). The easternmost cast has a salinity maximum close to a neutral density of $\gamma^n = 27.70\ \text{kg m}^{-3}$, but the salinity maximum rises to less dense surfaces as one moves along the tongue to the west. As explained by McDougall and Giles (1987), such a diapycnal migration of a salinity maximum

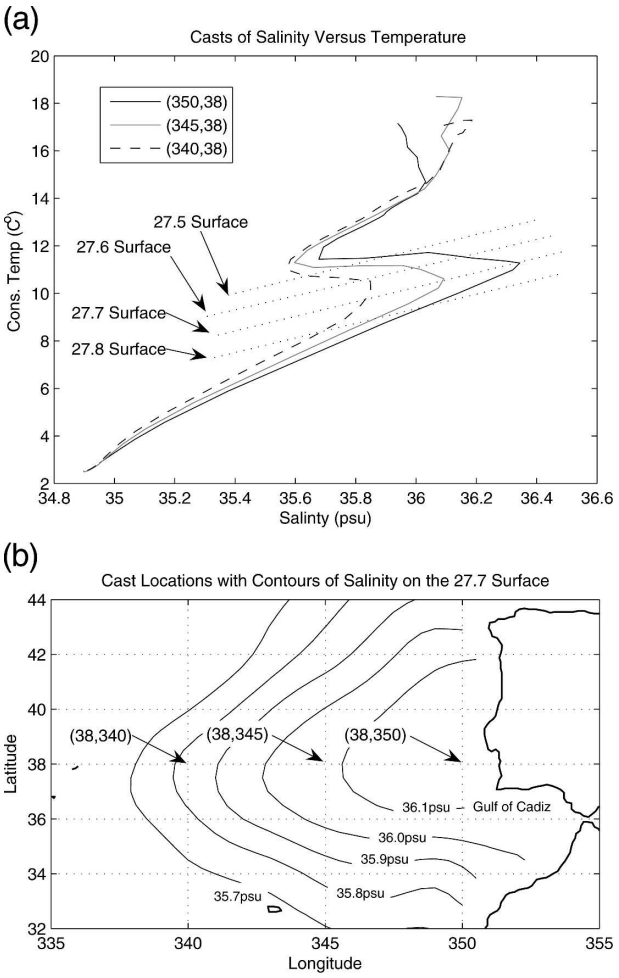

FIG. 1. (a) Salinity-conservative temperature diagram of three vertical "casts" of the atlas hydrography near the Gulf of Cadiz at locations illustrated in (b), which shows contours of potential temperature on the neutral density surface $\gamma^n = 27.70\ \text{kg m}^{-3}$. The four dashed lines in (a) are straight-line approximations to where the four neutral density surfaces lie on this figure.

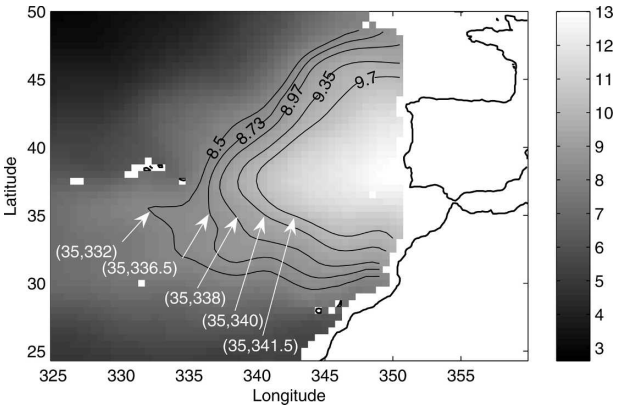

FIG. 2. Contours of Θ_0 on the $\gamma^n = 27.70\ \text{kg m}^{-3}$ density surface. These five contours define the westernmost edge of five areas, each of which extends eastward as far as 351°E. The color bar and contours are of potential temperature (°C).

should not automatically be interpreted as implying asymmetric vertical mixing processes since salinity itself is an asymmetric variable. Another way of looking at this issue is to form a salinity anomaly variable that represents the presence of Mediterranean Water with respect to a background North Atlantic water mass field that exists in the rest of the North Atlantic. This variable has isolines that rise about 15°C for every unit increase in salinity, and the maximum of this anomaly variable does not so obviously move across isopycnals.

Based on the curvature of the casts at (38°N, 350°E) and (38°N, 345°E) we see that the peak salinity occurs at a density of approximately $\gamma^n = 27.65\ \text{kg m}^{-3}$ and take this to be the central neutral density of the Mediterranean outflow. We will henceforth consider the hydrography between neutral densities of 27.50 and $27.80\ \text{kg m}^{-3}$ in order to capture the majority of the outflow, consistent with the work of Baringer and Price (1997).

Looking closely at the S–Θ cast at (38°N, 350°E) we notice a "dented" section between the neutral densities 27.6 and 27.7. This dent represents a discontinuity in the curvature and is consistent with the observation that the Mediterranean Water does tend to have a strong signature on two distinct density surfaces (sometimes called two "cores") close to the outflow region [as reviewed by Baringer and Price (1997)]. To minimize the influence of this vertical variation of S–Θ curvature we choose S_0 contours well away from the Gulf of Cadiz; that is, we choose contours that extend west of 340°E.

On the density surface $\gamma^n = 27.70\ \text{kg m}^{-3}$ we show (Fig. 2) the five S_0 contours that are used as bounds for five overlapping areas on this density surface. For the other density interfaces used in this study we chose S_0 contours at the locations of the arrow tips in Fig. 2, thus forming regions of roughly equivalent areas on each density surface. In this way we have chosen S_0 contours passing through longitudes 332°, 336.5°, 338°, 340°, and 341.5°E, each at 35.5°N, on neutral density surfaces of 27.5, 27.55, 27.6, 27.65, 27.7, 27.725, 27.75, 27.775, and 27.8. Thus we have five sets of areas on each of eight density layers, giving 40 equations of the form (20). Note that the density intervals were chosen to give approximately equal vertical spacing (dbar) between layers. We have limited the area of our calculations to being west of 351°E in order to exclude the region of complicated geometry and complex mixing processes close to the Strait of Gibraltar and north of the Iberian

TABLE 1. Table of contour values S_0 and Θ_0; the values of salinity (psu) and temperature (°C) coming into each layer from the Mediterranean Sea, S_M and Θ_M; and the length, L, along these contours of the largest area of Fig. 2.

Neutral density layer (kg m^{-3})	S_0	Θ_0	S_M	Θ_M	A (m^2 $\times$ 10^{12})	L (m $\times$ 10^6)
27.50–27.55	35.531	9.520	36.072	11.701	2.199	3.955
27.55–27.60	35.536	9.239	36.124	11.614	2.245	3.969
27.60–27.65	35.542	8.950	36.178	11.524	2.259	4.041
27.65–27.70	35.547	8.652	36.236	11.441	2.233	4.090
27.70–27.75	35.543	8.388	36.299	11.361	2.246	4.074
27.75–27.775	35.530	8.161	36.336	11.256	2.272	4.011
27.775–27.80	35.510	7.902	36.320	11.034	2.286	3.972
27.80–27.825	35.480	7.588	36.247	10.582	2.320	3.882

Peninsula. Factoring in these areas would marginally increase the surface area and contour length, but we would expect it to produce a negligible change in our results. Table 1 gives the areas and lengths along the S_0 and Θ_0 contours corresponding to the largest area on Fig. 2. The salinity and conservative temperature of the Mediterranean Water entering each layer, S_M and Θ_M, are taken to be the maximum values close to (36°N, 352°E), which is close to the easternmost point of our dataset and the position of maximum salinity and conservative temperature.

Baringer and Price (1997) describe the Mediterranean outflow as it descends from the Strait of Gibraltar. After the bulk of the mixing and entrainment has occurred, the volume flux of "Mediterranean Water" into the North Atlantic is estimated as 1.52 Sv (Sv $\equiv 10^6$ m^3 s^{-1}). Based on this paper we take this as the transport of the outflow once it has stopped actively entraining and that this outflow was distributed vertically over a range of neutral densities of 0.75 kg m^{-3} centered at approximately $\gamma^n = 27.65$ kg m^{-3}. Plots of salinity and temperature on our surfaces affirm this range of densities. Hence we approximate the distribution of the flow as a sine wave with zeros at neutral densities of 27.65 $\pm$ 0.375 kg m^{-3} and an integral between this region equalling 1.52 Sv. Figure 3 shows the volume flux that is assumed to flow into each density bin of width 0.05 kg m^{-3}. We use only the central half of the density range shown in Fig. 3, and the actual volume flux into our densest three layers is half that shown, simply because those layers have a density "width" of only 0.025 kg m^{-3}. Baringer and Price's estimate has been gathered from mooring data, and, although it is indeed not exact, we take it as a known for the purposes of this study. The sensitivity of changes in Q of $\pm$10% is explored later in this section, and it is emphasized that the solutions for K and D are proportional to the magnitude of Q.

In Table 2 we present the three relevant coefficients that appear in (20) for each of the 40 areas considered (5 contours times 8 layers). The upper set of 40 numbers are of $\int_{S_0} h(\Delta S \nabla_\gamma \Theta - \Delta\Theta \nabla_\gamma S) \cdot \mathbf{n}\, dl$, which multiplies K in (20); the middle set are of $A\langle(\Theta_z^u - \Theta_z^l)\Delta S - (S_z^u - S_z^l)\Delta\Theta\rangle$, which multiplies D in (20); and the third set of coefficients are of $Q(\Delta\Theta[S_M - S_0] - \Delta S[\Theta_M - \Theta_0])$, which multiplies F in (20).

We argue in the appendix that F lies in the range $0.85 < F < 1.0$, or $F = 0.925 \pm 0.075$, and in what follows actually take F to be unity because the uncertainty in estimating Q is considered to be larger than that associated with estimating F. Hence we will consider the left-hand side of (20) to be known for each of our 40 equations. As a first step, one might assume that the diffusivities K and D do not vary in space, either laterally or vertically. Then we have 40 equations in just two unknowns and find that the overdetermined least squares solution is $K = 481 \pm 114$ m^2 s^{-1} and $D = 2.2 \times 10^{-5} \pm 7.5 \times 10^{-5}$ m^2 s^{-1}. The estimate of the standard error of K was found by substituting $D = 2.2 \times 10^{-5}$ m^2 s^{-1} into each of the 40 equations, and, similarly, the estimate for the standard error of D was found by substituting $K = 481$ m^2 s^{-1} into each of the

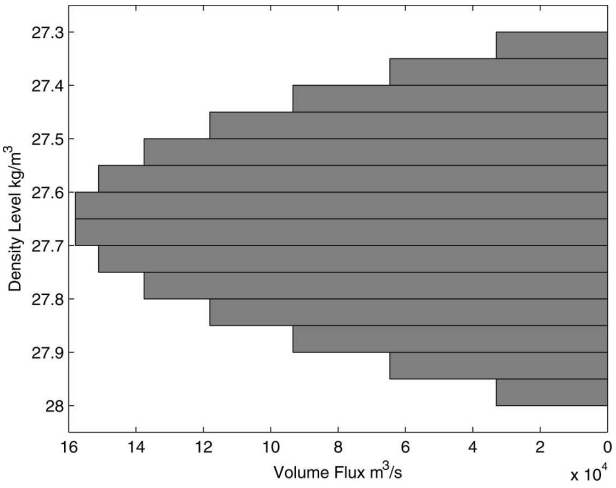

FIG. 3. The volume flux of Mediterranean Water flowing into the North Atlantic as a function of neutral density layer (following Baringer and Price 1997).

TABLE 2. Based on the hydrography and the volume flux of Mediterranean Water (from Baringer and Price 1997), the coefficients of K and D in (20) (the first two parts of the table) and the left-hand side of (20) (the third part of the table) for the 40 different control volumes we consider in this paper. The first two parts of the table have units: m psu K; the third has units: $m^3\ s^{-1}$ psu K.

	Longitude of contour				
Neutral density layer ($kg\ m^{-3}$)	332°E	336.5°E	338°E	340°E	341.5°E
	$\int_{S_0} h(\Delta S \nabla_\gamma \Theta - \Delta\Theta \nabla_\gamma S) \cdot \mathbf{n}\, dl$				
27.50–27.55	32.79	31.87	33.18	34.69	33.14
27.55–27.60	39.32	33.78	35.56	37.14	38.08
27.60–27.65	44.88	44.74	45.81	48.83	45.80
27.65–27.70	56.04	53.49	52.57	54.03	54.75
27.70–27.725	17.29	16.09	15.50	15.54	15.74
27.725–27.75	18.71	17.46	16.73	16.75	18.27
27.75–27.775	20.39	20.51	18.66	18.00	16.28
27.775–27.80	20.52	21.64	18.51	18.43	18.05
	$A\langle(\Theta_z^u - \Theta_z^l)\Delta S - (S_z^u - S_z^l)\Delta\Theta\rangle \times 10^{-7}$				
27.50–27.55	9.696	9.851	8.683	7.291	5.955
27.55–27.60	12.15	10.33	8.952	7.375	6.292
27.60–27.65	10.03	10.08	7.958	6.156	4.121
27.65–27.70	10.72	10.16	7.965	4.454	1.704
27.70–27.725	5.971	4.666	3.935	2.890	1.946
27.725–27.75	8.130	6.445	5.488	4.037	3.257
27.75–27.775	12.55	10.11	8.452	6.765	4.815
27.775–27.80	14.42	12.51	9.981	8.557	6.852
	$FQ(\Delta\Theta[S_M - S_0] - \Delta S[\Theta_M - \Theta_0])$				
27.50–27.55	21 514	19 846	19 077	16 504	14 024
27.55–27.60	27 531	23 237	21 661	18 686	16 454
27.60–27.65	30 899	28 099	25 701	22 184	18 199
27.65–27.70	34 900	32 309	29 210	24 477	20 507
27.70–27.725	9457	8635	7905	6778	5576
27.725–27.75	9446	8713	8143	7023	6259
27.75–27.775	10 338	9171	8574	7634	5723
27.775–27.80	10 124	9262	8028	7343	6352

40 equations. The spatially constant diapycnal diffusivity, at $D = 2.2 \times 10^{-5} \pm 7.5 \times 10^{-5}\ m^2\ s^{-1}$ while being relatively small, is also rather poorly known in that even its sign is in doubt.

The rather uncertain value found for the spatially invariant diapycnal diffusivity raises the question of whether this is simply indicative of resolving power of the method and the hydrography or whether this result was indicative of a real variation of diffusivity in space. Noting that each of our 40 equations are simply linear relations between K and D, we plotted these 40 linear relations on the D–K diagram and noticed that the straight lines for the five contours from each density layer tended to intersect, while these points of (near) intersection are different from one layer to the next. This is illustrated in Fig. 4, which shows 10 such straight lines, 5 from each of two different layers. There is a strong tendency for the lines from an individual layer to nearly cross at a point: This strongly suggested that the method has sufficient resolving power to be able to estimate both D and K and that these diffusivities were not constant in the vertical.

Hence, we performed least squares fits, assuming that the diffusivities K and D were constant along each layer. In this way we performed eight such fits with five equations in each fit, and the resulting values of the diffusivities for the eight layers are shown in Fig. 5 and Table 3. The errors bars σ_D and σ_K for these diffusivities are obtained by taking the constant value of the other diffusivity (either K or D) in each layer and the five equations, (20), then give five values of the diffusivity in question (either D or K) from which the standard deviation is calculated.

The first thing to notice in Fig. 5 is that the diffusivities are all positive and they vary quite smoothly from one layer to the next rather than varying randomly in the vertical. The standard error of these diffusivities is quite small, especially for the dianeutral diffusivity D. The error bars here do not reflect any uncertainty in the estimate of the effective transport FQ but rather the resolving power of the signature of the tracer patterns in the averaged hydrography to be able to distinguish between dianeutral and epineutral diffusion for a given FQ. We find the rather small standard errors of these diffusivities remarkable and surprising.

The vertical structure of the diapycnal diffusivity in

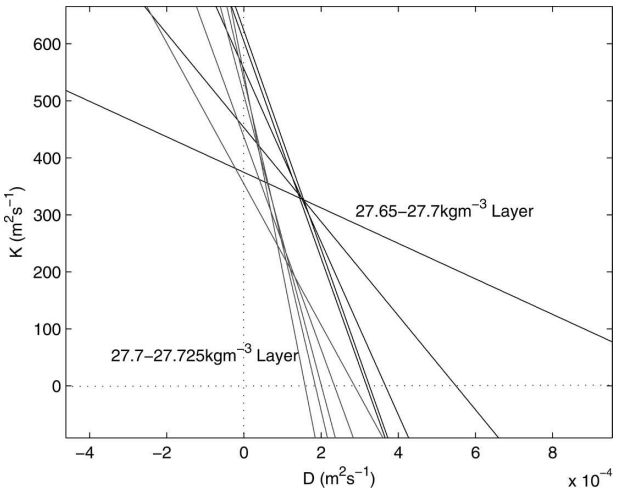

FIG. 4. Ten examples of the linear equation (20) relating K and D (for the known values of FQ). The five lines that nearly coincide at the larger values of D and K are for the five contours of the 27.65–27.70 density layer, while the other five lines are for the 27.70–27.725 density layer.

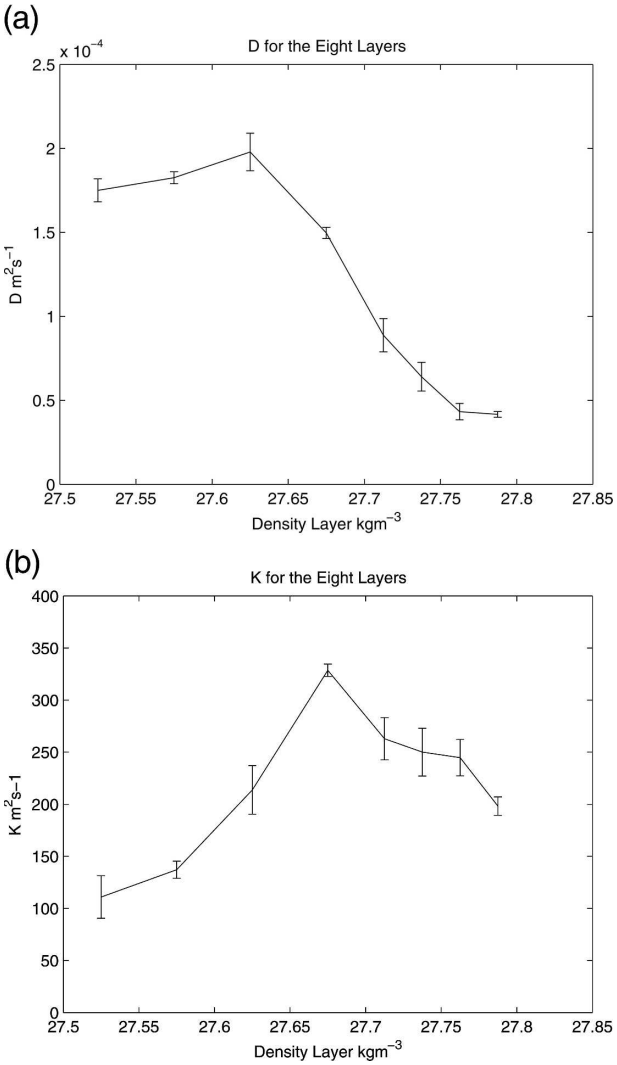

FIG. 5. The (a) dianeutral diffusivity D and (b) epineutral diffusivity K for each density layer, determined assuming that both D and K are constant in each layer.

Fig. 5 exhibits a rather strong vertical variation from the core of the Mediterranean Water at $\gamma^n \approx 27.65$ kg m^{-3} where we find $D \approx 2 \times 10^{-4}$ m^2 s^{-1} toward deeper layers where the diapycnal diffusivities are seen to be about 0.5×10^{-4} m^2 s^{-1}. The epineutral diffusivities in this region of about 200 m^2 s^{-1} are much less than values nearer the sea surface but may be appropriate for this depth and region of the ocean. The orderly progression of both D and K with density is probably due to our use of the rather smooth hydrographic atlas data. Nevertheless, the small error bars on these diffusivities give us some hope that the idea of carefully choosing the reference temperatures and salinities and the ratios $\Delta S/\Delta\Theta$ in order to achieve the three properties described in section 2 may add skill to the determination of diffusivities in a more general inverse problem. There have been few observational studies of diffusivity in this region. In the North Atlantic Tracer Release Experiment (NATRE) region (25°N, 332°E), which is farther to the south and west of the area that we are considering, Ferrari and Polzin (2005) found $D \approx 10^{-5}$ m^2 s^{-1} and $K \approx 300$ m^2 s^{-1}. Our diapycnal diffusivity is a factor of about 10 greater than this and our epineutral diffusivity is about a factor of 2 smaller.

The relative importance of vertical and epineutral diffusion in explaining the effective lateral advection of Mediterranean Water through this part of the North Atlantic is indicated in Fig. 6. For each density layer we have used the least-squares-determined values of D and K to evaluate the fraction of the right-hand sides of the five equations, (20), that are due to vertical and epineutral diffusion. The regular progression of the lines in this figure is probably indicative of the smoothed nature of the hydrographic atlas data and the fact that the areas that we consider are cumulative so that the properties of the area might be expected to vary slowly. The dashed curve with the smallest fractional influence is the curve for the largest horizontal area (the westernmost contour), and the successive dashed lines are the contours proceeding to the east in a monotonic fashion. The opposite occurs for the full lines where the curve for the smallest fractional influence is the easternmost contour with the smallest horizontal area. Perhaps this regular progression indicates that there may be more information that can be extracted using this technique, such as trying to determine a spatial variation of the diffusivities inside each isopycnal layer. We have not attempted to do so in this exploratory study but note

TABLE 3. The diffusivities and their standard errors, with both D and K being treated as constant along each density layer. The eight layers are treated independently, and in each layer D and K are determined as the only two unknowns in an overdetermined set of five equations corresponding to the five different S_0 contours.

Neutral density layer (kg m^{-3})	D (m^2 s^{-1})	σ_D (m^2 s^{-1})	K (m^2 s^{-1})	σ_K (m^2 s^{-1})
27.50–27.55	17.5×10^{-5}	0.7×10^{-5}	110.9	20.4
27.55–27.60	18.3×10^{-5}	0.4×10^{-5}	137.1	8.25
27.60–27.65	19.8×10^{-5}	1.1×10^{-5}	213.7	23.3
27.65–27.70	15.0×10^{-5}	0.3×10^{-5}	328.6	5.92
27.70–27.725	8.88×10^{-5}	1.0×10^{-5}	262.9	20.3
27.725–27.75	6.41×10^{-5}	0.9×10^{-5}	250.0	23.0
27.75–27.775	4.32×10^{-5}	0.5×10^{-5}	244.6	17.5
27.775–27.80	4.17×10^{-5}	0.2×10^{-5}	198.3	8.82

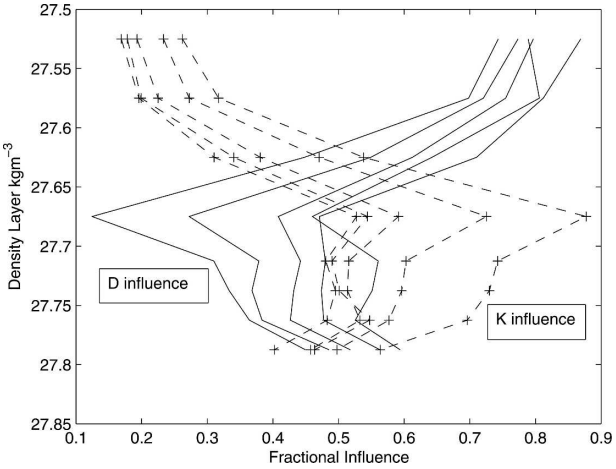

FIG. 6. Using the values of D and K for each layer (from Table 3 and Fig. 5), the fractional contribution to the right-hand side of (20) from the term in D and the term in K for each of the five equations for each layer.

that, if we took the diapycnal diffusivity to decrease and the lateral diffusivity to increase away from the Gulf of Cadiz, this would be consistent with the differences in D and K between the NATRE site and our study region, as well as tending to have the five solid lines and five dashed lines in Fig. 6 collapsing onto single full and dashed lines.

We have checked the robustness of the technique presented in this paper by varying the values of the vertical difference in salinity and conservative temperature, ΔS and $\Delta\Theta$, separately by $\pm 10\%$ and then redoing the analysis. These four separate changes typically resulted in changes to the diffusivities of less that 1%, confirming that the terms (22) and (23) that we neglected in arriving at our conservation equation (20) are indeed small. Another assumption built into our results is the vertical structure of the volume flux of Mediterranean Water entering the North Atlantic. Since we examined only the central range of densities between neutral densities of 27.50 and 27.80, we effectively chose the volume flux per unit density interval to be nearly constant (see Fig. 3). Nevertheless, this is an assumption. and our results in each density layer are directly proportional to the volume flume entering the layer.

Another key assumption that we have made is to use the same diapycnal turbulent diffusivity for heat as for salt. This is equivalent to assuming that the diapycnal mixing is caused by isotropic turbulent mixing. Another assumption would be to take the ratio of the diapycnal fluxes of heat and salt to be that in salt fingers, but we have not attempted this here.

4. Diffusivities from Hallberg Isopycnal Model data

Model output from the same region of the North Atlantic as in section 3 has been gained from the Hallberg Isopycnal Model (HIM; Hallberg 2000). There are three main advantages of using HIM as a means of testing the accuracy of the method already applied to the atlas data: First, HIM is one of the few global circulation models to impose a *volume* transport through the Strait of Gibraltar. If only temperature and salinity fluxes are allowed through the strait the overall dynamics of the region are changed (Griffies et al 2005). Second, by utilizing a density coordinate system HIM avoids the unwanted mixing effects caused by the Veronis effect in z-coordinate GCMs (Veronis 1975). Third, as HIM is already on density surfaces, we avoid any error implicit in interpolating to density surfaces from a Cartesian grid of Θ, S, and p values. The HIM output used is the time average of the final 20 years of a 100-yr coupled experiment The model uses a σ_2-coordinate system with a total of 49 layers in the vertical and a horizontal resolution of 1° of longitude and latitude. The model is not eddy resolving, has an isopycnal diffusivity (K_{model}) of 600 m^2 s^{-1}, and employs a Richardson number (Ri) dependent vertical diffusion scheme that results in high vertical diffusivities [D_{model} $O(10^{-4})$] in regions of high Ri and relaxes to a background profile [depth-dependent $O(10^{-5})$] in the deep ocean. For the region explored by this study, D_{model} is close to 1.8×10^{-5} (i.e., within 10%).

The model stores velocity, advective flux, and diffusive fluxes of heat and salt in the meridional, zonal, and vertical directions. From the advective fluxes close to the Strait of Gibraltar we are able to assign a specific Q value to each layer in the vertical. Layers 36.0, 36.1, 36.2, and 36.3 are chosen as they represent the majority of the volume of the salt tongue and are bounded by

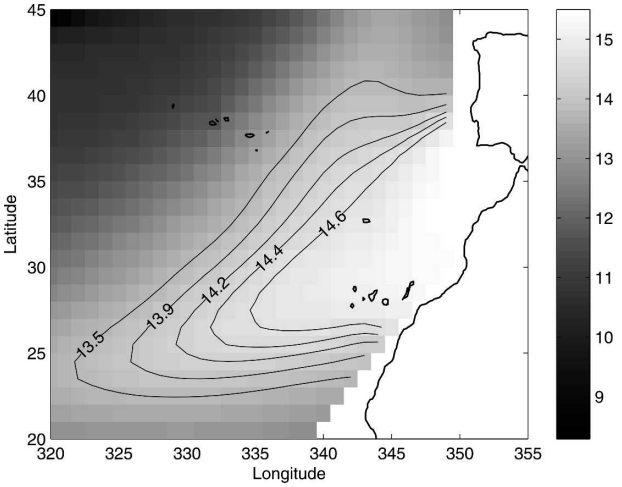

FIG. 7. Contours of Θ_0 on the $\sigma_2 = 36.2$ kg m^{-3} density layer. These five contours define the westernmost edge of five areas. The easternmost edge is also shown where the flux into a given area is the sum of flux values through that boundary. The shade bar and contours are of potential temperature (°C).

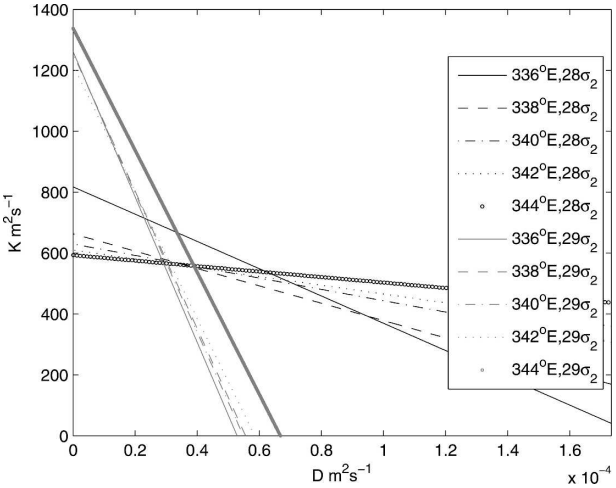

FIG. 8. Ten examples of the linear equation (20) relating K and D (for the known values of FQ). Unlike the hydrographic atlas data (from Gouretski and Koltermann 2004), the lines representing (20) for the 29 σ_2 layer are close to parallel, suggesting that K and D should not be determined for each layer independently.

five surfaces equally spaced in density coordinates. Contours are chosen such that they pass through latitude 35.5°N and longitudes 336°, 338°, 340°, 342°, and 344°E. One downside of using model output is the unsmoothed nature of the data close to the continents. Along both the Portuguese and Moroccan coasts the pressures on density surfaces are quite variable, and this data is removed by defining an eastern boundary to the region that is 1°–2° from the coast. The inflow Q may now be approximated as the volume flux through that boundary rather than simply the flux out of the Gulf of Cadiz. The region in question is shown in Fig. 7 along with the position of all five contours on the 36.2 σ_2 layer.

Once again we have five sets of areas, now on each of four density layers, giving 20 equations of the form (20). Our initial overdetermined least squares solution is $K = 586 \pm 131$ m^2 s^{-1} and $D = 3.42 \times 10^{-5} \pm 1.79 \times 10^{-5}$ m^2 s^{-1}. It was found in the previous section that, when K and D were solved for each layer, much greater precision resulted, and it is thus pertinent to look to the intersection of lines in K–D space formed by each equation. A comparison between the lines formed by areas on both the 36.2 σ_2 and 36.3 σ_2 layers is shown in Fig. 8. While the lines formed by the 36.2 σ_2 layer compare well to those of the hydrographic atlas, each having varied slopes and intersecting within a small range, the lines formed on the 36.3 σ_2 layer are close to parallel. Clearly the ratio of coefficients in front of K and D in Eq. (20) varies little within each extra area on the 29.0 σ_2 layer, and thus not enough information is present to solve for K and D within that layer individually. Possible explanations for this may lie in the averaging problem mentioned earlier and the fact that there may be something implicit in HIM that maintains a constant ratio between the K and D coefficients in (20), which is not observed in the real Mediterranean outflow.

We chose to solve for K and D for each set of equivalently sized areas in the vertical, making the assumption that K and D are constant on each set. The values obtained along with the average values used in HIM for these regions are displayed in Table 4 and Figs. 9a and 9b (for $F = 1$), and these results show that the diagnosed K and D values vary little throughout this region. The model values also vary little in space but differ from those diagnosed by around a factor of 2 in the D case and 20%–50% in the K case.

In the above calculations the assumption that $FQ = Q$ has been made, as was the case in section 3, where an estimate for Q was all that was known. Since time-averaged volume fluxes are known at every point in space of the HIM data, we examine whether the inclusion of a better approximation for F will improve our ability to estimate K and D. In section 2, it was shown that FQ can be thought of as the average of the flow into the layer from the Mediterranean and the flow out through the contour that bounds it. Making this modification to the left-hand side of (20), the overall least squares estimates become $K = 625 \pm 109$ m^2 s^{-1} and $D = 2.52 \times 10^{-5} \pm 1.87 \times 10^{-5}$ m^2 s^{-1}, and K and D for each set of areas in the vertical are shown in Figs. 9a

TABLE 4. The diffusivities determined from HIM output and their standard errors, with both D and K being treated as constant for a set of areas in the vertical. The five contour locations are treated independently, and in each contour D and K are determined as the only two unknowns in an overdetermined set of four equations corresponding to the four different layers.

Longitude of contours at 35.5°N	D ($m^2\ s^{-1}$)	σ_D ($m^2\ s^{-1}$)	K ($m^2\ s^{-1}$)	σ_K ($m^2\ s^{-1}$)
336°E	3.34×10^{-5}	1.29×10^{-5}	612	153
338°E	3.52×10^{-5}	1.12×10^{-5}	569	131
340°E	3.25×10^{-5}	1.48×10^{-5}	582	135
342°E	3.13×10^{-5}	2.18×10^{-5}	588	146
344°E	3.65×10^{-5}	2.52×10^{-5}	573	167

and 9b. Here K adjusts slightly upward, while D is reduced by 30%–50%, bringing the model D value well within the standard deviation of that diagnosed by this inverse technique. With $F = 1$, the gain or loss of volume within each layer is not accounted for. In the above case, diapycnal fluxes create a reduction in the outflow volume of each layer, and constructing an inverse model without taking this into account gives an overestimate of the vertical diffusivities. When advective fluxes are incorporated into the inverse model through the variable F, a better estimate for D results, with little change to our estimate for the lateral diffusivity K.

5. Summary

By taking a carefully chosen linear combination of the conservation statements of volume, salinity, and conservative temperature, we have arrived at (20), which is effectively a conservation equation for the variable $\Delta S(\Theta - \Theta_1) - \Delta\Theta(S - S_1)$ where the offset values Θ_1 and S_1 are chosen to be the volume-averaged conservative temperature and salinity of the control volume, and the vertical differences ΔS and $\Delta\Theta$ are the area-averaged differences between the values at the upper and lower interfaces bounding a density layer. Because of its careful construction, the vertical gradient of this variable is on average zero, and hence dianeutral advection makes a negligible contribution to (20), as does the vertical gradient of the dianeutral diffusivity. Rather, the process of dianeutral mixing enters (20) only as the average of the dianeutral diffusivity at the upper and lower interfaces. In addition, this dianeutral diffusion term is proportional to the vertical curvature of the S–Θ diagram, which is much less subject to numerical noise than is traditionally the case when estimating second derivatives such as S_{zz} and Θ_{zz}. These advantages were the motivation for forming this rather careful linear combination of the conservation equations.

Needler and Heath (1975) analyzed the Mediterranean Water signature in the North Atlantic using a salinity anomaly measured at fixed values of potential temperature with respect to a linear S–θ relation. Diapycnal advection of this salinity anomaly was ignored in their study. This can be justified at the central density of the Mediterranean Water because there this type of salinity anomaly shares the same important property as our (21), namely that its vertical gradient is zero, so the effect of diapycnal advection can be neglected. Above and below the central density, the vertical gradient of the salinity anomaly is nonzero, and our technique,

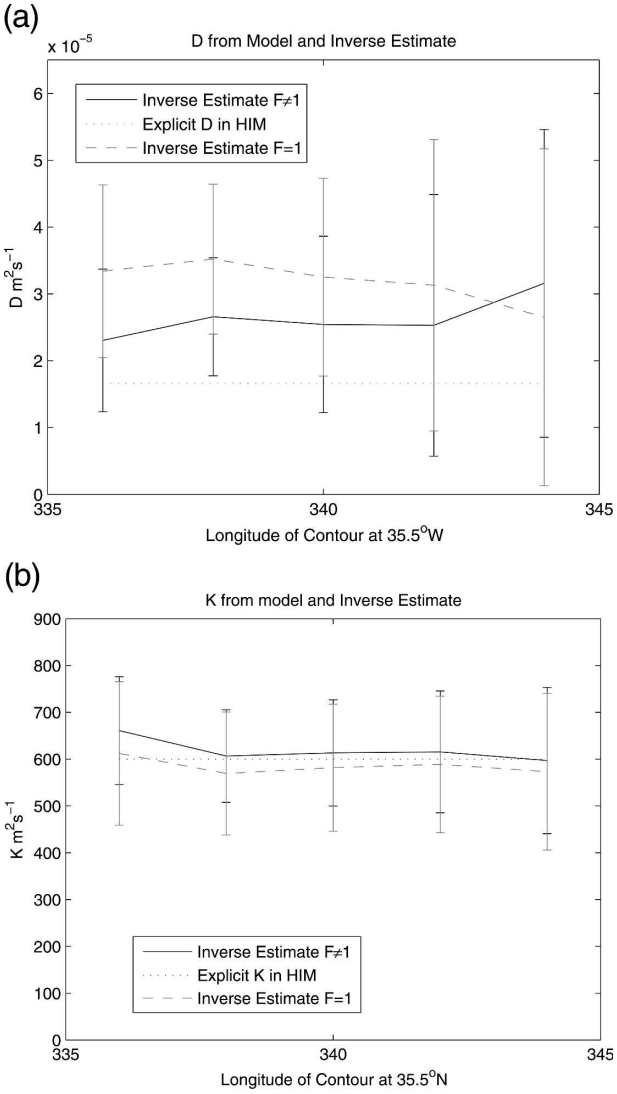

FIG. 9. (a) The dianeutral diffusivity D for each set of areas in the vertical, determined assuming that both D and K are constant within all the areas in the vertical, assuming $F = 1$ (gray and dashed), $F \neq 1$ (black), and the explicit value in HIM (small dashed). (b) The epineutral diffusivity K for each set of areas in the vertical, determined assuming that both D and K are constant within all the areas in the vertical, assuming $F = 1$ (gray and dashed), $F \neq 1$ (black), and the explicit value in HIM (dashed).

which has a different ratio $\Delta\Theta/\Delta S$ for each density layer, is preferred.

Before using this technique in a more general inverse model of ocean hydrography we have applied it to the hydrography in the eastern North Atlantic, which has two very important advantages for our purposes. First, the volume flux entering the North Atlantic from the Mediterranean Sea can be taken as known and regarded as steady and, second, the hydrographic data has a very obvious Mediterranean Water signature. The extra terms (A1)–(A3) due to dianeutral advection and the vertical variation of the dianeutral diffusivity that should appear in (20) have been shown to have a negligible influence on the results of our study.

The method seems able to distinguish between the effects of epineutral and dianeutral diffusion on the dilution of the Mediterranean Water signature in the eastern North Atlantic. Also, the overdetermined least squares "inversion" gives dianeutral and epineutral diffusivities that vary smoothly in the vertical. The data examined here is from an ocean atlas (Gouretski and Koltermann 2004), and it remains to be seen how the method performs on unaveraged ocean hydrography. In this region of the ocean meddies are known to transport a significant amount of heat and salt laterally (Armi and Zenk 1984), and it is clear that this mechanism will not be well parameterized as diffusion. The analysis of the HIM data provided a further test of the ideas. It is not clear why the coefficients of the two diffusivities were so closely proportional along one of the model layers but, in any case, the technique recognized this and attached large uncertainties to the diffusion coefficients. We are encouraged by the results of this technique in this rather special region and plan to apply it as a more general inverse technique in the ocean, where one does not have an a priori estimate of the volume flux entering one side of the box.

Acknowledgments. We thank Drs. Susan Wijffels and Nathan Bindoff for insightful and helpful comments on a draft of this paper. This work contributes to the CSIRO Climate Change Research Program and has been partially supported by the CSIRO Wealth from Oceans Flagship.

APPENDIX

The Three Extra Terms in Eq. (20)

There are three other terms that arise from the last three terms of (18) (and the corresponding equation for conservative temperature) that should appear in (20) but have been omitted because we can show that they are small. These three terms are the spatial integrals of

$$-(e^u - e^l)\left\{\left[\frac{1}{2}(\Theta^u + \Theta^l) - \Theta_1\right]\Delta S - \left[\frac{1}{2}(S^u + S^l) - S_1\right]\Delta\Theta\right\}, \quad \text{(A1)}$$

$$-\frac{1}{2}(e^u + e^l)[(\Theta^u - \Theta^l)\Delta S - (S^u - S^l)\Delta\Theta], \quad \text{(A2)}$$

and

$$(D^u - D^l)\left[\frac{1}{2}(\Theta_z^u + \Theta_z^l)\Delta S - \frac{1}{2}(S_z^u + S_z^l)\Delta\Theta\right]. \quad \text{(A3)}$$

Equation (A1) can be written as

$$(e^u - e^l)\left[\frac{1}{2}(S^u + S^l) - S_1\right]\left[\Delta\Theta - \frac{\beta}{\alpha}\Delta S\right], \quad \text{(A4)}$$

where β and α are the saline contraction and thermal expansion coefficients (because the variations of salinity and temperature along density surfaces are related by $\beta\nabla_\gamma S = \alpha\nabla_\gamma\Theta$). The last term in (A4) does not vary much because the ratio β/α is a slowly varying function of space. Now consider varying S_1 between S_M and S_0. At one extreme the middle term in (A4) is positive throughout the whole area of integration, while for the other extreme choice of S_1 the middle term in (A4) is negative over the whole area. When area integrated, (A1) and (A4) will then very likely give either a positive or a negative integral for these extreme choices. It is likely that the value of the salinity offset that makes the area average of (A1) zero will be close to the area-averaged salinity. This is the value of S_1 that we seek since we wish to minimize the influence this term can have on (18). Spatial correlations between $(e^u - e^l)$ and the middle term in (A4) will cause the value of S_1 that zeros on the spatial average of (A1) to be different from the spatially average salinity. However, unless these spatial correlations are very strong, we feel justified in taking S_1 to be close to the area-averaged salinity; that is, we assume $S_1 \approx 0.5\langle S^u + S^l\rangle$ and $\Theta_1 \approx 0.5\langle\Theta^u + \Theta^l\rangle$. In any case, we will assume that the lateral and vertical diffusivities do not vary along each layer, so in that sense it is consistent to make this assumption for S_1, as it is also effectively an assumption about minimum spatial variation, namely of $(e^u - e^l)$. Bearing in mind the geometry of the isohalines of the Mediterranean Water as it spreads into the North Atlantic, if $S_1 \approx 0.5\langle S^u + S^l\rangle$ then we take the ratio of salinities in (16) as

$$0.25 < \frac{[S_1 - S_0]}{[S_M - S_0]} < 0.5. \quad \text{(A5)}$$

With values of c between 0.7 and 1.0, the resulting range of F is approximately $0.85 < F < 1.0$.

Notice that the choice of the constant salinity S_1 appears in the conservation equation (20) only through its influence on F and in one of the additional terms, namely term (A1). Since we will ignore this term, it is important to ensure that it is small, and a suitable choice of S_1 will ensure that this term is zero. While we are unsure of this value of S_1, we believe that it lies in a range that implies that F is between 0.85 and 1.0. Hence we conclude that the price of ignoring the contribution of (A1) to (20) is merely to suffer this relatively small uncertainty in the magnitude of the product FQ.

Now we consider the influence of the ignored terms (A2) and (A3) on (20). Since $0.5(S_z^u + S_z^l) \approx (S^u - S^l)/h$, (A2) and (A3) can be combined as

$$-\left[\frac{1}{2}(e^u + e^l) - (D^u - D^l)/h\right][(\Theta^u - \Theta^l)\Delta S - (S^u - S^l)\Delta\Theta]. \quad \text{(A6)}$$

The area integral of the second pair of brackets in (A6) is zero by definition so that, if the first pair did not vary in space in this layer, then the area integral of (A6) would be zero. Because of spatial correlations between the two pairs of brackets, the area average of (A6) can be nonzero. However, if we compare the terms involving diapycnal diffusivities in our main equation in (20) and in (A6) we see that in (20) this term involves the *sum* of these diffusivities multiplied by the curvature of the S–Θ curve, which is of one sign in this region, while in (A6) we have the *difference* in the diffusivities multiplying a term whose area average is zero. Hence we do not expect the neglect of (A6) to be important. If we leave one of ΔS or $\Delta\Theta$ as given by (19) and vary the other, then one could achieve a zero value for the area integral of (A6). This is the value of $\Delta S/\Delta\Theta$ that we need to choose so as to ensure that (A2) and (A3) do not contribute to (20), although we have no way of knowing exactly this value of $\Delta S/\Delta\Theta$. We will perform our method with three different values of $\Delta S/\Delta\Theta$ that span a variation of 20% and will find that the results are not sensitive to this uncertainty.

In summary, we believe that the errors involved in ignoring the contributions of the three terms (A1)–(A3) to (20) can be made to be small and will not materially affect the results. Ignoring (A1) causes us to suffer some uncertainty in F and hence in the effective lateral advection FQ along the layer, while the effect of ignoring the terms in (A2) and (A3) will be shown to be small by empirically varying the ratio $\Delta S/\Delta\Theta$ that we use in (20) away from the value set by (19).

REFERENCES

Armi, L., and W. Zenk, 1984: Large lenses of highly saline Mediterranean water. *J. Phys. Oceanogr.,* **14,** 1560–1576.

Baringer, M. O., and J. F. Price, 1997: Mixing and spreading of the Mediterranean outflow. *J. Phys. Oceanogr.,* **27,** 1654–1677.

Ferrari, R., and K. L. Polzin, 2005: Finescale structure of the *T*–*S* relation in the eastern North Atlantic. *J. Phys. Oceanogr.,* **35,** 1437–1454.

Ganachaud, A., and C. Wunsch, 2000: Improved estimates of global ocean circulation, heat transport and mixing from hydrographic data. *Nature,* **408,** 453–457.

Gouretski, V. V., and K. P. Koltermann, 2004: WOCE global hydrographic climatology. Berichte des Bundesamtes für Seeschifffahrt und Hydrographie Tech. Rep. 35/2004, 49 pp.

Griffies, S. M., 2004: *Fundamentals of Ocean Climate Models.* Princeton University Press, 518 pp.

——, and Coauthors, 2005: Formulation of an ocean model for global climate simulations. *Ocean Sci.,* **1,** 45–79.

Hallberg, R. W., 2000: Time integration of diapycnal diffusion and Richardson number–dependent mixing in isopycnal coordinate ocean models. *Mon. Wea. Rev.,* **128,** 1402–1419.

Jackett, D. R., and T. J. McDougall, 1997: A neutral density variable for the world's oceans. *J. Phys. Oceanogr.,* **27,** 237–263.

McDougall, T. J., 1984: The relative roles of diapycnal and isopycnal mixing on subsurface water mass conversion. *J. Phys. Oceanogr.,* **14,** 1577–1589.

——, 1987: Thermobaricity, cabbeling, and water-mass conversion. *J. Geophys. Res.,* **92,** 5448–5464.

——, 1991a: Water mass analysis with three conservative variables. *J. Geophys. Res.,* **96,** 8687–8693.

——, 1991b: Parameterizing mixing in inverse models. *Dynamics of Oceanic Internal Gravity Waves: Proc. 'Aha Huliko'a Hawaiian Winter Workshop,* Honolulu, HI, University of Hawaii at Manoa, 355–386.

——, 2003: Potential enthalpy: A conservative oceanic variable for evaluating heat content and heat fluxes. *J. Phys. Oceanogr.,* **33,** 945–963.

——, and A. B. Giles, 1987: Migration of intrusions across isopycnals, with examples from the Tasman Sea. *Deep-Sea Res.,* **34A,** 1851–1866.

——, and P. C. McIntosh, 2001: The temporal-residual-mean velocity. Part II: Isopycnal interpretation and the tracer and momentum equations. *J. Phys. Oceanogr.,* **31,** 1222–1246.

——, and D. R. Jackett, 2005a: The material derivative of neutral density. *J. Mar. Res.,* **63,** 159–185.

——, and ——, 2005b: An assessment of orthobaric density in the global ocean. *J. Phys. Oceanogr.,* **35,** 2054–2075.

McIntosh, P. C., and S. R. Rintoul, 1997: Do box inverse models work? *J. Phys. Oceanogr.,* **27,** 291–308.

Needler, G. T., and R. A. Heath, 1975: Diffusion coefficients calculated from the Mediterranean salinity anomaly in the North Atlantic Ocean. *J. Phys. Oceanogr.,* **5,** 173–182.

Sloyan, B. M., and S. R. Rintoul, 2000: Estimates of area-averaged diapycnal fluxes from basin-scale budgets. *J. Phys. Oceanogr.,* **30,** 2320–2341.

Veronis, G., 1975: The role of models in tracer studies. *Numerical Models of Ocean Circulation,* National Academy of Science, 133–146.